RSC Advances

ROYAL SOCIETY OF CHEMISTRY

www.rsc.org/advances

RSC Advances

RSCPublishing

ARTICLE

Design and synthesis of non-crystallizable, low-T_g polysiloxane elastomers with functional epoxy groups through Anionic Copolymerization and Subsequent Epoxidation

Cite this: DOI: 10.1039/xoxxoooooox

Received ooth January 2012,
Accepted ooth January 2012

DOI: 10.1039/xoxxoooooox

www.rsc.org/

Yang Meng[a,b], Junfeng Chu[a,b], Jiajia Xue[a,b], Chaohao Liu[a,b], Zhen Wang[c] and Liqun Zhang[a,b,*]

Although polysiloxane elastomers have many merits, their fast crystallization at low temperature is problematic in some fields. In this study, a novel non-crystallizable, low-T_g epoxidized polysiloxane (ESR) with functional epoxy groups in side chains was designed and synthesized though two steps: (i) the preparation of poly(methylvinylsiloxane) (SR) by anionic ring-opening copolymerization of 2,4,6,8-tetramethyl-2,4,6,8-tetravinyl cyclotetrasiloxane and octamethylcyclotetrasiloxane, and (ii) the subsequent epoxidation of the SR. Reaction kinetic studies demonstrated that the epoxidation of SR was a second-order reaction and more than 90% of the double bonds were converted into epoxy groups during the epoxidation. Despite a slight increase in the T_g of ESRs as the content of epoxy groups increased, the low-temperature performances of ESRs were greatly improved because of the inhibition of the crystallization of polysiloxane chains. Surprisingly, the ESRs also showed higher thermal degradation temperatures than the traditional poly(dimethylsiloxane) did. The excellent low-temperature performance and high degradation temperatures endowed the ESR with great potential as elastic materials in the aerospace where the materials have to undergo very high and low temperature.

1 Introduction

Polysiloxane elastomers (silicone rubbers) are among inorganic and semi-inorganic polymers having an alternating silicon-oxygen backbone chain with organic side chains.[1-3] Polysiloxane elastomers show many excellent properties, such as high flexibility, high thermal stability, optical transparency, biocompatibility, and high gas permeability. Due to these merits, polysiloxane elastomers attracts considerable interest, from both industry and academia, and play important roles in the aerospace industry, automobile industry, electronic industry, and biological applications.[4-9]

Despite having many excellent properties, polysiloxane elastomers show some weaknesses, which affect their practical use in some fields. One major drawback of polysiloxane elastomers is their fast crystallization at low temperature. Although polysiloxane elastomers have very low glass transition temperature (T_g), most of them will become stiff and cannot be used as elastic materials at temperatures far higher than their T_g.[10-12] For instance, poly(dimethylsioxane) (PDMS), the most extensively studied polysiloxane by far, shows its T_g at about -125 ℃ but its melting point is as high as about -40 ℃.[13] Because of the crystallization, polysiloxane elastomers cannot make full use of the advantage of their very low T_g and their applications, especially the aerospace where the materials have to undergo very low temperature, are seriously limited. In addition to the crystallization, the low mechanical properties, weak oil resistance, and poor hydrophobicity are also problematic for most of polysiloxane elastomers.[14-20] In addition, some properties of polysiloxane elastomers, such as thermal stability, still need to be improved to meet the applied requirements. Therefore, designing new polysiloxane elastomers with high performances is of great importance.

Chemical modification is a useful method to alter and optimize the properties of polymers. Of all the well-known chemical modifications of polymers, epoxidation is one of the most promising and advantageous methods due to its relatively mild reaction conditions and significant improvement in the properties of the polymers.[21-24] Epoxidation of polymers is typically performed with organic peracids (such as m-chloroperbenzoic acid and magnesium monoperoxyphthalate) or a combination of a transition metal catalyst and a co-oxidant (such as H_2O_2 and t-BuOOH).[25,26] Theoretically, all polymers containing unsaturated carbon bonds can be epoxidized under appropriate reaction conditions. The introduction of polar, functional epoxy groups into polymer chains can improve the properties of the final polymer, such as oil resistance, damping property, and gas barrier property.[27-30] Owing to the formation of hydrogen bonds or covalent bonds between epoxy groups and inorganic fillers (e.g., silica), the presence of epoxy groups

can enhance the interaction between polymers and inorganic fillers, leading to a good dispersion of fillers and improved mechanical properties of polymer composites.[31,32] Epoxidation of bacterial polyesters carried out by Park et al.[33] showed that epoxidation can also affect the thermal properties, such as raising the glass transition temperature, decreasing the melting temperature, and inhibiting crystallization. Moreover, the epoxy groups can react with other groups, such as amino and carboxyl, and endow polymers with great potential for further chemical modification.[34,35]

Based on the merits of epoxidized polymers, the introduction of epoxy groups into polysiloxane elastomer chains would be meaningful because the epoxy groups would inhibit the crystallization of polysiloxane elastomers and endow the polysiloxane elastomers with reactive groups for further chemical modification. The polar and reactive epoxy groups would be also beneficial for improving the compatibility of polysiloxane with other polar polymers and enhancing the interaction between polysiloxane and fillers. A few studies on the synthesis of silicone-epoxy resins or silicone-epoxy monomers have been reported.[36-39] In these studies, the epoxy groups were mainly introduced into silicones by the hydrosilylation at the presence of catalyst, e.g. platinum. The silicones should have Si-H in side or end of the silicone chains, and the molecular weights of the silicones were usually low, resulting in a low molecular weight of the silicone-epoxy products. Yang et al.[40] reported a method of synthesizing silicone-epoxy polymer by the condensation of silicone-epoxy monomer and dimethyldiethoxysilane, but the molecular weight of the product was still very low. Eckberg et al.[41] prepared a silicone-epoxy polymer by epoxidation of the silicone containing C=C groups; however, the silicone containing C=C groups still needed to be prepared first by the hydrosilylation. In addition, the above reported silicone-epoxy monomers or linear silicone-epoxy polymers are often used for reins or coatings. The use of silicone-epoxy polymers as elastomers, to our knowledge, has not been reported.

In this study, we bring out a strategy to synthesize epoxidized polysiloxane (ESRs) elastomers, in which we firstly synthesized poly(methylvinylsiloxane) (SRs) via common anionic ring-opening polymerization based on 2,4,6,8-tetramethyl-2,4,6,8-tetravinyl cyclotetrasiloxane and octamethylcyclotetrasiloxane, and then conducted an epoxidization reaction. The peracid, m-chloroperbenzoic acid (MCPBA), was used to synthesize ESR because MCPBA has proved to be very effective for the epoxidation of unsaturated polymers.[42-44] Chloroform, because of its solubility in both SR and MCPBA, was selected as the reaction medium for the epoxidation. A series of non-crystallizable, low-T_g epoxidized polysiloxane (ESRs) with high molecular weights were successfully prepared. These ESRs have excellent low-temperature performance and high thermal degradation temperatures.

2 Experimental

2.1 Materials and chemicals

Octamethylcyclotetrasiloxane (D_4, $C_8H_{24}O_4Si_4$, purity ⩾98%) was purchased from Shanghai Jiubang Chemical Co., Ltd., China. Decamethyltetrasiloxane ($C_{10}H_{30}O_3Si_4$, purity ⩾ 97%), 2,4,6,8-tetramethyl-2,4,6,8-tetravinylcyclotetrasiloxane (V_4, $C_{12}H_{24}O_4Si_4$, purity ⩾ 97%) and tetramethylammonium hydroxide (TMAOH, $C_4H_{13}NO$, 25% aq. soln.) were purchased from J&K Scientific, Ltd., China. 3-Chloroperbenzoic acid (MCPBA, $C_7H_5ClO_3$, 75%) was purchased from Aladdin Reagent Co., Ltd., China. D_4 and V_4 were purified by distillation for two times and other chemicals were used as received without further purification. Polydimethysiloxane (PDMS) with the vinyl content of 0.15 mol% was purchased from Chenguang Chemical Research Insititute, China.

2.2 Synthesis of tetramethylammonium silanolate

To improve the compatibility of the initiator (TMAOH) with the monomers (D_4 and V_4), tetramethylammonium silanolate containing 1.0 wt% TMAOH was synthesized as initiator from D_4 and TMAOH. Into a 100-mL three-neck glass flask equipped with a condenser, a thermometer, and a nitrogen sparging device, 30.0 g of D_4 and 1.2 g of TMAOH solution were added. The system was then heated to 50 °C, vacuumized to 0.1 kPa, and dehydrated by nitrogen sparging for 1 h. Then the system was heated to 80 °C to start the reaction and vacuumized to 20.0 kPa to remove the generated H_2O. The reaction was terminated after 1 h and the system was then vacuumized to 0.1 kPa until the product became transparent. The chemical equation is shown in Scheme 1 (Step 1).

2.3 Synthesis of poly(methylvinylsiloxane)

Into a 100-mL three-neck glass flask equipped with a condenser, a thermometer, and a mechanical agitator, D_4, V_4, and decamethyltetrasiloxane in given molar ratios (0.95:0.05:0.0006, 0.90:0.10:0.0006, 0.85:0.15:0.0006, and 0.80:0.20:0.0006) were added. After the mixture was heated to 50 °C and vacuumized to 0.1 kPa for 1 h, the tetramethylammonium silanolate (1.0 wt% of the mixture) was added. The system was then purged with high purity nitrogen, stirred at 250 rpm, and heated to 110 °C to start the reaction. After 1.5 h, the reaction was terminated by heating the system to 180 °C, at which the tetramethylammonium silanolate was "decatalyzed" to trimethylamine.[45] Then the system was vacuumized to 0.1 kPa to remove the cyclic oligomers and the generated trimethylamine. After 2 hours, a transparent poly(methylvinylsiloxane) (SR) was obtained (see Fig. S1). The products with the molar ratios of D_4 to V_4 of 0.95:0.05, 0.90:0.10, 0.85:0.15, and 0.80:0.20 were named SR-5, SR-10, SR-15, and SR-20, respectively. For all SRs, the molecular weight was determined by GPC and the practical content of vinyl groups was measured by the bromine-iodometric technique according to GB/T 1676-1981. The chemical equation of the polymerization is shown in Scheme 1 (Step 2).

2.4 Epoxidation of poly(methylvinylsiloxane)

A 1.3 equiv sample (based on the vinyl groups in poly(methylvinylsiloxane)) of MCPBA was added into a 1000-mL round-bottom flask containing 18 g of poly(methylvinylsiloxane) dissolved in 600 mL of chloroform. The reaction was allowed to proceed under constant, gentle stirring at 25°C for 96 h, and then the solution was slowly poured into 2.4 L of cooled methanol. The precipitated polymer was washed with methanol twice and dried in a vacuum oven at 50 °C for 24 h. Then a transparent epoxidized polysiloxane (ESR) with random structure was obtained (see Fig. S1). The products from the epoxidation of SR-5, SR-10, SR-15, and SR-20 samples were named ESR-5, ESR-10, ESR-15, and ESR-20, respectively. The chemical equation of epoxidation is shown in Scheme 1 (Step 3).

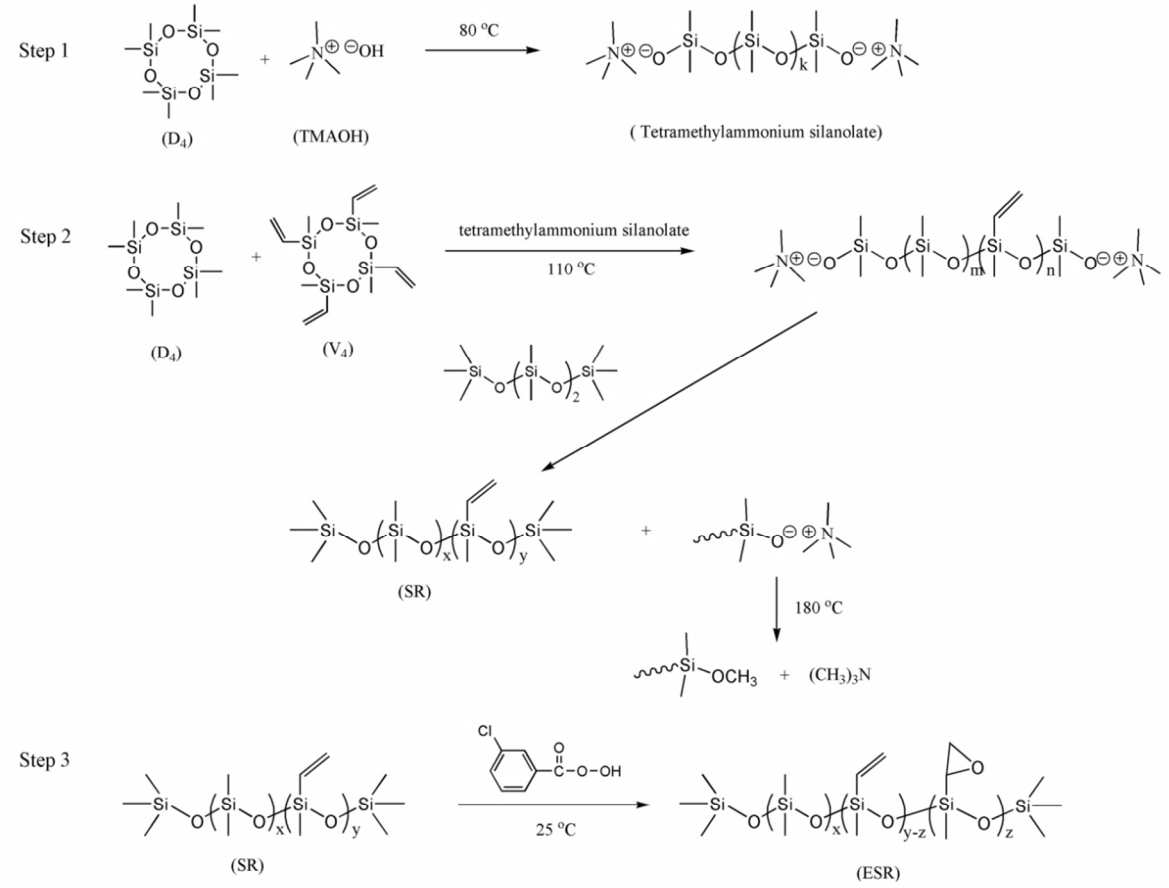

Scheme 1. The synthesis route of ESR.

2.5 Preparation of crosslinked silica/PDMS composites and silica/ESR composites.

The PDMS (or ESR) and additives were mixed by a 6 in. two-roll mill according to the formulation given in Table 1. The compound was cured in a XLB-D 350 × 350 hot press (Huzhou Eastmachinery Co., China) under 15 MPa at 160 °C for its optimum cure time t_{90}, which corresponds to the time when the degree of the crosslinking reaches to 90% (see Fig. S2). The optimum curing time was determined by a disk oscillating rheometer (P3555B2, Beijing Huanfeng Chemical Machinery Experimental Factory, China). During the curing, the peroxide DBPMH was decomposed to form radicals at high temperature. These generated radicals can reacted with the residual –CH=CH_2 or the –CH_3 of the polysiloxane chains to form polysiloxane radicals. The polysiloxane radicals then react with each other to form crosslinks.[46]

Table 1. The formulation for crosslinked silica/PDMS composites and silica/ESR composites.

Ingredients	Amount (phr) [b]
PDMS (or ESR)	100
Silica (Degussa A200)	40
Hydroxyl silicone oil	2
DBPMH[a]	0.1

[a] 2,5-bis(tert-butylperoxy)-2,5-dimethylhexane (93%).
[b] phr stands for parts per 100 parts of silicone rubber by weight.

2.6 Measurements and characterization

2.6.1 Nuclear magnetic resonance (NMR) spectroscopic analysis

^{1}H NMR spectra and ^{1}C NMR spectra were recorded at a frequency of 400 MHz with $CDCl_3$ as solvent by using a Bruker AV400 NMR spectrometer (Bruker, Germany).

2.6.2 Fourier transform infrared spectroscopy (FTIR) analysis

The FTIR spectra of D_4, V_4, SR, and ESR were recorded with a resolution of 4 cm^{-1} and the signal averaged over 32 scans on a Fourier transform infrared spectrometer (Tensor 27, Bruker Optik Gmbh Co., Gemany).

2.6.3 Gel permeation chromatography (GPC)

The molecular weights of SR and ESR were determined by GPC measurements on a Waters Breeze instrument equipped with three water columns (Styragel HT3_HT5_HT6E) using tetrahydrofuran as the eluent (1 mL/min) and a Waters 2410 refractive index detector.

2.6.4 Differential scanning calorimetry (DSC)

DSC measurements of SR and ESR were carried out on a Mettler-Toledo differential scanning calorimeter. A polystyrene standard was used for calibration. The samples were accurately weighed and sealed in aluminum crucibles. The samples were cooled to -145 °C at a cooling rate of 10 °C/min, maintained at -145 °C for 10 min, and then heated to 30 °C at a heating rate of 10 °C/min.

2.6.5 Thermogravimetric analysis (TGA)

Thermogravimetric (TGA) measurements were carried out on a STARe system TGA/DSC1 thermogravimeter (Mettler-Toledo International Inc., Switzerland) with a cooling water circulator. The testing was done under a flowing nitrogen atmosphere (20 mL/min). All the samples used in the TGA measurements were similar in weight (10 ± 1 mg) and heated from 30 to 800 °C at a heating rate of 10 °C/min.

2.6.6 Dynamic mechanical properties

Dynamic mechanical properties of ESR composites were measured by a dynamic mechanical analyzer (DMAVA3000, 01 dB Co., Ltd., France). The specimens were 15 mm long, 15 mm wide, and about 1 mm thick. Tension mode was used for DMA test. The temperature dependence of the loss factor tan δ and storage modulus were measured in the range -135 to 30 °C at a frequency of 10 Hz and a heating rate of 3 °C/min.

2.6.7 Measurement of epoxy value (EV)

The epoxy value of ESR (molar content of epoxy groups per 100 g of ESR) was measured by the HCl-THF method. About 0.5 g of ESR was dissolved in 20 mL of THF, and then 10 mL of HCl/THF solution (0.25 mol/L of H^+) was added into the ESR solution. After 30 min, 5 drops of phenolphthalein indicator were added, and the excess HCl was titrated by NaOH (0.10 mol/L). The epoxy value (EV, mol/100g) of ESR was calculated by equation (1):

$$EV = \frac{(V_0 - V) \times C}{W} \times 100 \qquad (1)$$

where C is the concentration of NaOH standard solution (mol/L), V_0 is the blank comsumption of NaOH standard solution (L), V are the sample consumption of NaOH standard solution (L), and W is the weight of the sample used (g).

2.6.8 Cold-resistance of ESR

The cold-resistance of ESR was determined by cold-resistance-factor tester (RH-7040, Renheng Machinery Plant, Yangzhou, China) according to Chinese standard GB/T 3866-2008. A cylindrical sample (Φ10 mm×10 mm) of silica/ESR composite was compressed 20% at room temperature and then put into ethanol, which was cooled by dry ice to a setting temperature (-50 °C,-60 °C, and -70°C). After the sample had been immersed in ethanol for 5 min, the compressive load was removed and the height of the cylindrical sample was measured after 3 min. The cold resistance factor under compression (K_c) was calculated by equation (2):

$$Kc = \frac{h_2 - h_1}{h_0 - h_1} \qquad (2)$$

where h_0, h_1, and h_2 are the height of the sample before compression, the height of the sample after compression, and the height of the sample 3 min after the compressive load is removed, respectively.

3 Results and Discussion

3.1 Synthesis and structure of poly(methylvinylsiloxane) (SR)

Poly(methylvinylsiloxane) with different contents of vinyl groups as precursors of ESRs were synthesized by the anionic ring-opening polymerization of D_4 and V_4 initiated by tetramethylammonium silanolate. Fig. 1 shows the ^{1}H NMR spectrum and ^{13}C NMR spectrum of SR-20. ^{1}H NMR ($CDCl_3$, 400MHz) δ ppm: 5.90-6.05, 5.74-5.84 (-CH=CH_2); 0.12-0.16, 0.05-0.09 (-CH_3). ^{13}C NMR ($CDCl_3$, 400MHz) δ ppm: -0.08-0.08 (Si-CH_3); 135.8-136.1 (CH_2=); 131.6-132.0 (-CH=).

Table 2 shows the number-average molecular weights (M_n), weight-average molecular weights (M_w), and molecular weight distributions of SRs with different molar ratios of V_4 to D_4. The number-average molecular weights are in the range 200,000-300,000, which is similar to those of commercially available PDMS. Although anionic ring-opening polymerization method was adopted to synthesize SRs, the molecular weight distributions of SRs are a little broad. As the molar ratio of V_4 to D_4 increases, the molecular weight distributions of SRs increase from 1.67 to 2.46. The broad molecular weight distributions of SRs could be ascribed to the rearrangement reaction and chain transfer reaction during the polymerization, as shown in Scheme 2.[47] In the process of chain growth, the active center can bite back to form different cyclic oligomers (Scheme 2(a)) or attack the other polysiloxane chains to form new active center (Scheme 2(b)), leading to randomization of polysiloxane chains and broad molecular weight distributions.

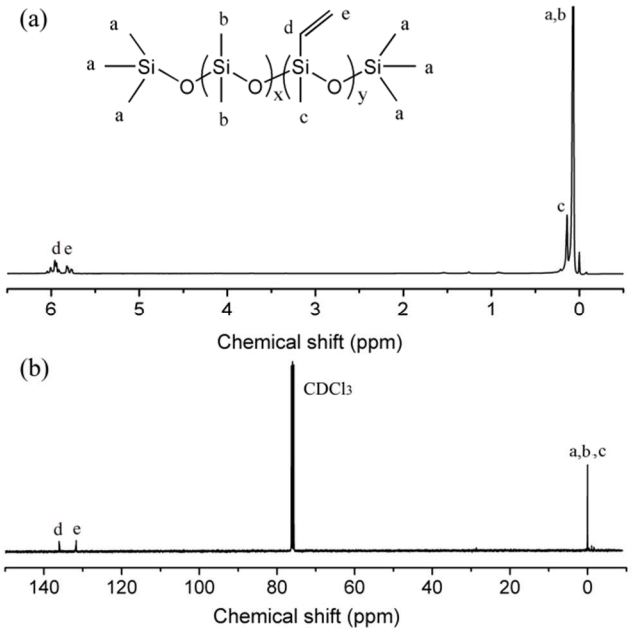

Fig. 1. NMR spectra of poly(methylvinylsiloxane) (SR-20): (a) ^{1}H NMR spectrum and (b) ^{13}C NMR spectrum.

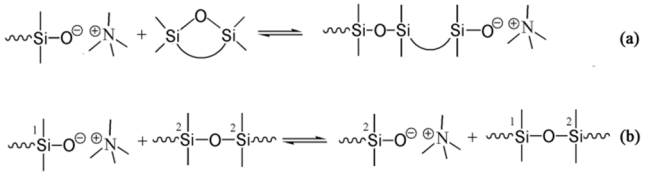

Scheme 2. The (a) rearrangement reaction and (b) chain transfer reaction during the synthesis of SRs.

Additionally, we measured the vinyl content of SR by the bromine-iodometric technique, considering that the practical vinyl content would be different from the theoretical vinyl content because some cyclic oligomers existed at the end of polymerization. Table 2 shows that the measured vinyl content of a SR is higher than the theoretical value calculated from the molar ratio of D_4 to V_4, but the

difference between the measured vinyl content and the theoretical value is very small.

3.2 Synthesis and structure of epoxy-poly(methylvinylsiloxane)

The epoxidation of olefins is typically performed with organic peracids or a combination of a transition metal catalyst and a co-oxidant. In this study MCPBA was used for the epoxidation of SR. Fig. 2 shows the ^{1}H NMR spectrum and ^{13}C NMR spectrum of ESR-20. ^{1}H NMR ($CDCl_3$, 400MHz) δ ppm: 5.90-6.05, 5.74-5.84 (-CH=CH_2); 2.84-2.90, 2.63-2.70, 2.09-2.15 (Si-CH-CH_2) 0.05-0.09, 0.09-0.13 (-CH_3). ^{13}C NMR ($CDCl_3$, 400MHz) δ ppm: 29.8-30.0, 43.0-43.2 (Si-CH-CH_2); -1.01--1.05, -0.08-0.08, -1.01--1.05 (Si-CH_3). In Fig. 2(a), the resonances at 5.98 and 5.82 ppm assigned to the -CH=CH_2 protons, become very weak in the ^{1}H NMR spectrum, indicating that most of the vinyl groups have been converted into epoxy groups during the epoxidation. The high conversion of -CH=CH_2 can be also verified by the change in the signal of the methyl groups: the signal at 0.14 ppm corresponding to the c-type methyl groups (Fig. 1(a)) almost disappears and a new signal at 0.11 ppm assigned to the d-type methyl groups appears in the ^{1}H NMR spectrum of ESR-20 (Fig. 2(a)). In the ^{13}C NMR spectrum of ESR-20 shown in Fig. 2(b), the signals assigned to the epoxy groups appear at 41.0 and 30.0 ppm, but those assigned to the vinyl groups, which should appear at 136.1 and 131.7 ppm (Fig. 1(b)), cannot be seen. The ^{13}C NMR results are consistent with the ^{1}H NMR results, further confirming that most of the vinyl groups have been converted to epoxy groups.

To calculate the epoxidation yield of ESRs with different contents of vinyl groups, two methods—^{1}H NMR and titration—were used. In the ^{1}H NMR method, the unchanged integral of CH_3 was selected as the primary integral 1 for all the samples, and the epoxidation yield was calculated from the integrals of the –CH=CH_2 signals before and after epoxidation (see Fig. S3). In the titration method, the epoxidation yield was calculated from the ratio of measured epoxy values (EV) to theoretical EV. The epoxidation yields, epoxy contents, and EV of the various ESR samples are shown in Table 3. The epoxidation yields calculated by the ^{1}H NMR method and the titration method are similar, and are all higher than 90%. The molecular weights, molecular weight distributions and gel contents of the ESR samples are also listed in Table 3. Compared with those of SR, the molecular weights and molecular weight distributions of the ESR samples do not change much, indicating that there are not many side reactions, such as degradation, during the epoxidation. The gels contents of the ESR samples are very low, demonstrating that there is little crosslinking between the ESR macromolecular chains.

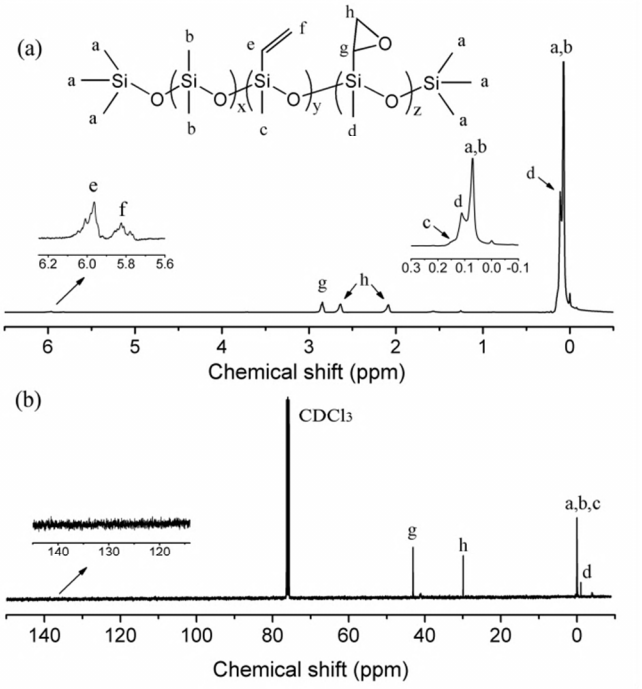

Fig. 2. NMR spectra of epoxy-poly(methylvinylsiloxane) (ESR-20): (a) ^{1}H NMR spectrum and (b) ^{13}C NMR spectrum.

Table 2. Molecular weights and vinyl contents of various SR samples.

Samples	D_4:V_4 (mol:mol)	M_n	M_w	M_w/M_n	Vinyl content (mol%)
PDMS	-	278,000	501,000	1.80	0.15
SR-5	95:5	269,000	449,000	1.67	5.4
SR-10	90:10	242,000	443,000	1.83	10.2
SR-15	85:15	221,000	514,000	2.46	15.6
SR-20	80:20	228,000	533,000	2.34	20.1

Table 3. Molecular weights and epoxidation yields of various ESR samples

.Samples	M_n	M_w	M_w/M_n	Gel (%)	Epoxidation yield by NMR (%)	Epoxidation yield by titration (%)	Epoxy content (mol%)[a]	Epoxy value (mol/100g)[a]
ESR-5	254,000	444,000	1.75	0	91.4	92.2	4.98	0.066
ESR-10	243,000	459,000	1.89	0.2	93.3	90.3	9.21	0.120
ESR-15	210,000	567,000	2.69	0.1	94.1	91.1	14.21	0.191
ESR-20	201,000	480,000	2.35	0.3	93.0	90.5	18.20	0.238

[a] epoxy content and epoxy value were calculated by titration.

3.3 FTIR spectra of D_4, V_4, SR, and ESR

Fig. 3 shows the FTIR spectra of D_4, V_4, SR-20, and ESR-20. IR (KBr, cm^{-1}): 3056 (=C-H, stretching vibration); 2965 (-CH_3, stretching vibration); 1598 (C=C, stretching vibration); 1408 (Si-C, asymmetric deformation vibration); 1262 (Si-C symmetric deformation vibration); 1087, 1020 (Si–O–Si, stretching vibration); 880 ( , ring vibration); 798 (Si-C, stretching deformation vibration). As can be seen from Fig. 3(d), the absorptions for double bonds are not clear after the epoxidation, illustrating that most of the double bonds have been converted to epoxy groups.

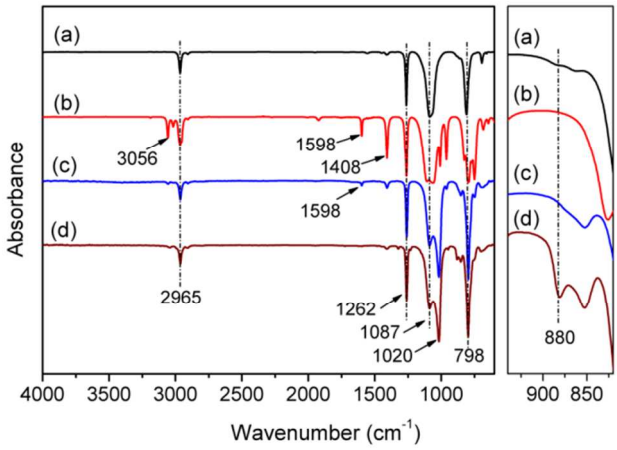

Fig. 3. FTIR spectra of (a) D_4, (b) V_4, (c) SR-20, and (d) ESR-20.

3.4 Kinetics of double bond conversion

Fig. 4 shows the degree of conversion of the double bonds into epoxy groups as a function of the reaction time for all the SR samples. At the same concentration of SR (3 g/100 mL), all the SR samples show the same trend of conversion as a function of reaction time: at the beginning of the epoxidation, all the samples show a high reaction rate because of the high concentrations of double bonds and MCPBA; after 24 h, the reaction rate decreases. Although the concentrations of SR are same, the vinyl contents of the SR samples are different. In other words, the concentrations of carbon double bonds and MCPBA are different at the beginning of epoxidation for different SR samples. Therefore, the epoxidation rates for the SR samples with different contents of vinyl groups should be different.

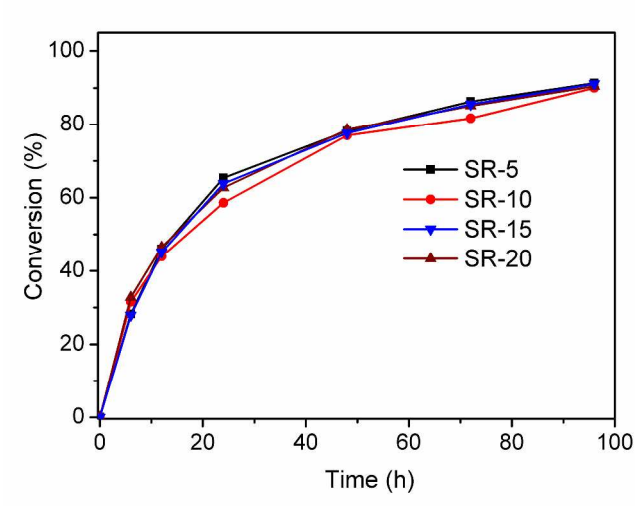

Fig. 4. Epoxidation rate of SR samples with different vinyl contents.

Some studies using MCPBA to prepare epoxides showed that the epoxidation reaction was initially second-order.[22,48] Assuming that the epoxidation reaction is second order, we can express the epoxidation rate for SR by equation (3):

$$\frac{d[epoxide]}{dt} = -\frac{d[C=C]}{dt} = k[C=C][MCPBA] \quad (3)$$

where k is the apparent second-order rate constant, and [*epoxide*], [*C=C*] and [*MCPBA*] are the concentration of epoxy groups, the concentration of vinyl groups, and the concentration of MCPBA, respectively. If we assume that one mole of carbon double bonds is converted into one mole of epoxy groups and the concentration of epoxy groups is x at time t, equation (3) can be expressed as

$$\frac{dx}{dt} = k(a-x)(b-x) \quad (4)$$

where a and b are the initial concentration of carbon double bonds and the initial concentration of MCPBA, respectively. Integration of equation (4) gives

$$\frac{1}{a-b} ln \frac{b(a-x)}{a(b-x)} = kt \quad (5)$$

Equation (5) can be further expressed in terms of the double bond conversion w:

$$\frac{1}{a-b} ln \frac{b(1-w)}{a(b/a-w)} = kt \quad (6)$$

Fig. 5 shows the results of Fig. 4 plotted in accordance with equation (6). For all the SR samples, the plots are linear, illustrating that the epoxidation of SR using MCPBA follows a second-order mechanism. In addition, the SR samples with different contents of vinyl groups show different apparent second-order rate constants (k), and the rate constant decreases with increasing the content of vinyl groups. The difference in k values is probably due to the different chemical structures of the ESRs. The commonly accepted mechanism for epoxy formation is the "butterfly" mechanism, which involves a cyclic polar process where a proton is transferred intramolecularly to the carbonyl oxygen with a concerted attack on the alkene by the hydrogen-bonded peracid.[49] The reaction rate depends significantly on the chemical structures of alkene and peracid; the electron-donating groups on the alkene and the electron-withdrawing groups on the peracid can accelerate the epoxidation rate.[50] Steric hindrance also plays an important role in the epoxidation rate.[51] Because the groups adjacent to the carbon double bonds are similar, the difference in k values should not be ascribed to the electron-donating ability of the adjacent groups but to the steric hindrance. For the SR samples with high contents of vinyl groups, the adjacent vinyl groups and the generated epoxy groups would hinder the epoxidation, resulting in a decrease in epoxidation rate.

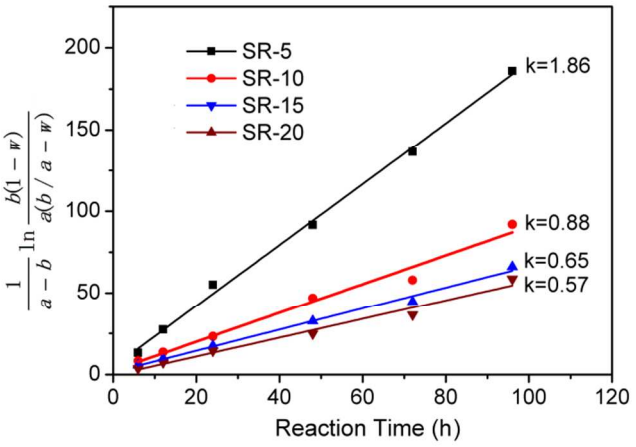

Fig. 5. Plots of $\frac{1}{a-b}\ln\frac{b(1-w)}{a(b/a-w)}$ versus reaction time.

3.5 Thermal transitions of SR and ESR

Thermal properties such as glass transition temperature (T_g) and crystallization are critical for elastomers because a polymer in the crystalline state or a polymer with a T_g higher than the temperature of use is not elastic. Fig. 6 shows the DSC curves of uncured PDMS and uncured SRs with different contents of vinyl groups. Despite showing a very low T_g (about -125.5°C), PDMS cannot be used as an elastomer at temperatures below -70 °C because of crystallization, as shown Fig. 6 (a). Using 61.3 J/g as the heat of fusion for PDMS,[52] we can calculate from the melting heat (ΔH_m) value for PDMS (29.1 J/g) that the degree of crystallinity for the PDMS used in this study is as high as 47.5%. As the vinyl content increases, the T_g of SR decreases slightly but the melting temperature (T_m) and the ΔH_m of SR (see Table S4) decrease significantly. The decrease in the T_m and ΔH_m demonstrates that the introduction of vinyl groups into PDMS decreases the regularity of the PDMS chains and affects the crystallization of PDMS. For SR-10, no exothermic peak of crystallization can be seen in the DSC cooling curve (Fig. 6(a)), indicating that the introduction of 10 mol% of vinyl groups into the PDMS side chains inhibits the crystallization thoroughly when the sample is cooled to -150 °C at 10 °C/min. However, an exothermic peak of cold crystallization ranging from -105 °C to -85 °C appears in the DSC heating curve (Fig. 6(b)) when the sample is heated from -150 °C to 20 °C, implying that the SR-10 is still crystallizable. For SR-15, neither an endothermic peak nor an exothermic peak can be seen in the DSC curve, suggesting that the crystallization of SR is completely inhibited. The very low T_g and noncrystalline behavior demostrate that SR containing a high content of vinyl groups has excellent low-temperature performance; however, this kind of SR is not an ideal polymer to be used as a low-temperature-resistant material because the large quantity of vinyl groups would adversely affect the thermal stability of the material.

When the vinyl groups in SR are converted into epoxy groups, the thermal properties such as glass transition temperatures (T_g) and crystallization show great changes. As shown in Fig. 7(a), when the content of epoxy groups reach 4.98 mol% (ESR-5), no exothermic peak of crystallization can be seen in the DSC cooling curves, indicating that the crystallization of ESR is inhibited when the sample is cooled to -150 °C at 10 °C/min. However, in the DSC heating curve of ESR-5 (Fig. 7(b)), an exothermic peak corresponding to cold crystallization appears in the range of -105 – -85 ° C when the sample is heated from -150 ° C to 20 ° C, implying that the ESR-5 is still crystallizable. In addition, ESR-5 shows a lower ΔH_m (21.2 J/g) than SR-5 does (see Table S4), suggesting that epoxy groups have a greater impact on the crystallization of PDMS than vinyl groups do, probably because of the larger steric hindrance of epoxy groups than that of vinyl groups. In the ESR samples with contents of epoxy groups higher than 9.21 mol% (e.g., ESR-10), neither an endothermic peak nor an exothermic peak can be seen in the DSC curves. The results from the DSC curve of ESR-10 further confirm that epoxy groups have a greater impact on the crystallization of polysiloxane than vinyl groups do in that an endothermic peak and an exothermic peak can be still seen in the DSC heating curve of SR-10 (Fig. 6(b)).

The introduction of epoxy groups into PDMS side chains also has a great impact on the T_g of PDMS. As shown in Fig. 7(b), the T_g increases substantially with increasing content of epoxy groups. Similarly, epoxidation was also reported to increase the T_g s of natural rubber, styrene butadiene rubber,

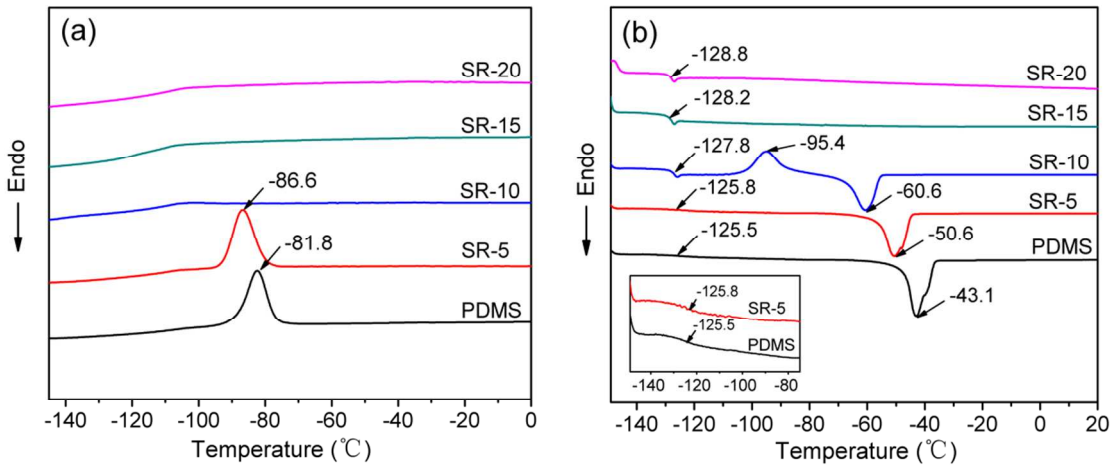

Fig. 6. DSC curves of PDMS and SRs with different contents of vinyl groups: (a) DSC cooling curves and (b) DSC heating curves.

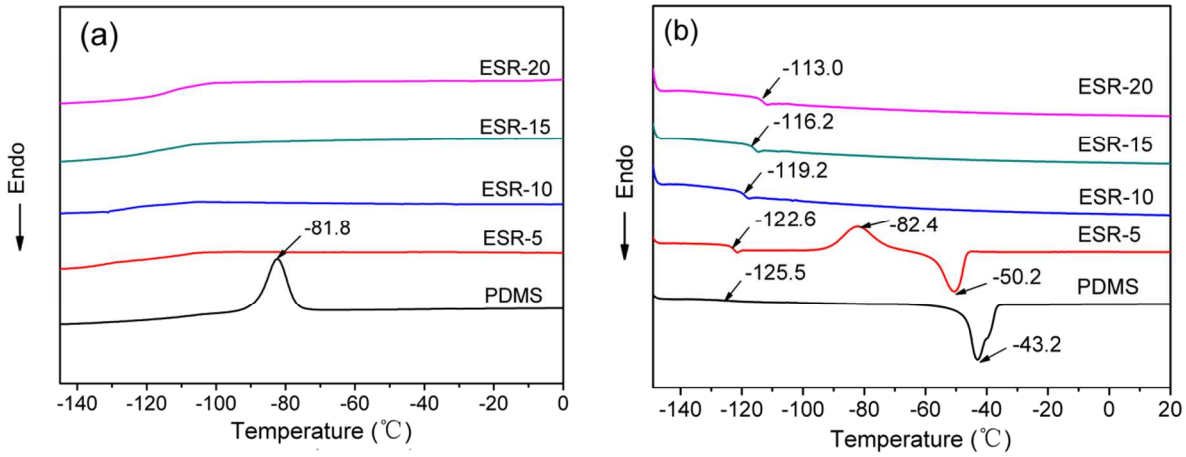

Fig. 7. DSC curves of PDMS and ESRs with different epoxy values: (a) DSC cooling curves and (b) DSC heating curves.

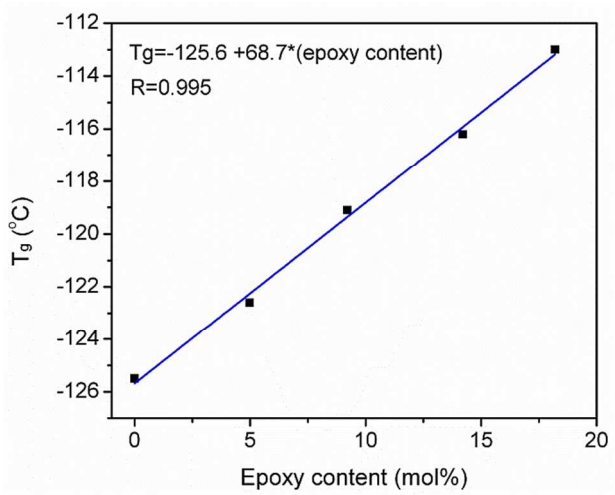

Fig. 8. Plot of T_g against epoxy content of ESR.

and other polymers such as polyesters.[33,39,57] The increase in T_g of ESR is attributed to the polar epoxy groups, which can increase the intramolecular interactions. Fig. 8 shows the plot of T_g versus epoxy content of ESR. The plot is linear and shows that the T_g increases by 0.69 °C as the content of epoxy groups increases 1 mol%. The increase rate of T_g with the content of epoxy groups is close to the that of other polymers reported in the literature.[33,57]

Dynamic mechanical analysis (DMA) can measure the phase transitions, such as melting, crystallization, alpha transition (glass), and beta transition of a material by vibrating the material sinusoidally at a constant frequency and small amplitude. For the determination of the phase transitions of materials, DMA is more sensitive than other measurements such as differential scanning calorimetry (DSC) and modulated differential scanning calorimetry (mDSC).[53] In this study, DMA was used to further investigate the phase transitions and low-temperature resistance of the crosslinked ESR composites with silica. Fig. 9(a) shows the elastic modulus (E') of ESR composites with different epoxy contents versus temperature. The E' of PDMS composite decreases as the temperature increases from -120 °C to -100 °C, and then decreases rapidly as the temperature increases from -50 °C to -40 °C. The changes of E' in the range of -120–-100 °C is ascribed to the glass transition, and that in the range of -50–-40 °C owns to the crystal melting. The change of E' in the range of -120–-100 °C is far smaller than that in the range of -50–-40 °C, implying that PDMS has a very high degree of crystallinity. In addition, E' can reflect the mechanical properties of PDMS composite; the sharp increase of E' in the range of -50–-40 °C means that the PDMS composite becomes very stiff and cannot be used as an elastic material below -50 °C. For ESR-5 composite, a sharp decrease of E' because of crystal melting can be still seen in the range of -60–-45 °C. However, the change of E' is lower than that for PDMS composite, implying a decrease in the degree of crystallinity. For ESR-10 composite, E' begins to decrease significantly at -115 °C because of glass transition, but then increases at approximately -95 °C owing to cold crystallization. As the temperature reaches -80 °C, the E' of ESR-10 composite begins to decrease again because of crystal melting. In the DSC curve of ESR-10 (Fig. 7), however, neither an endothermic peak nor an exothermic peak can be seen. Because DMA test was carried out at a constant frequency and a small amplitude, the cold crystallization of ESR-10 during the DMA test was probably induced by stress, which has been reported to accelerate the crystallization of polymers.[54-56] At a very low cooling rate, it was found that there is still an exothermic peak in the DSC cooling curve of ESR-10, but the ΔH_c is very low, indicating a low degree of crystallinity of ESR-10 (see Fig. S5). For ESR-15 composite, only a sharp decrease of E' corresponding to glass transition can be seen in Fig. 9(a), demonstrating an amorphous structure for ESR-15. The amorphous structure of ESR-15 can be further confirmed by the DSC cooling curve, in which none of exothermic peaks can be seen even at a very low cooling rate (see Fig. S5). At epoxy contents higher than 14.21 mol%, the temperature corresponding to the sharp decrease of E' increases because of the increase of T_g of ESR. Generally, the introduction of epoxy groups into the PDMS side chains can improve the low-temperature resistance of PDMS. As the epoxy content increases, the temperature corresponding to crystal melting decreases and the low-temperature resistance increases. Among these ESRs, however, ESR-15 should show the best low-temperature resistance because it is amorphous and has a lower T_g than ESR-20 does.

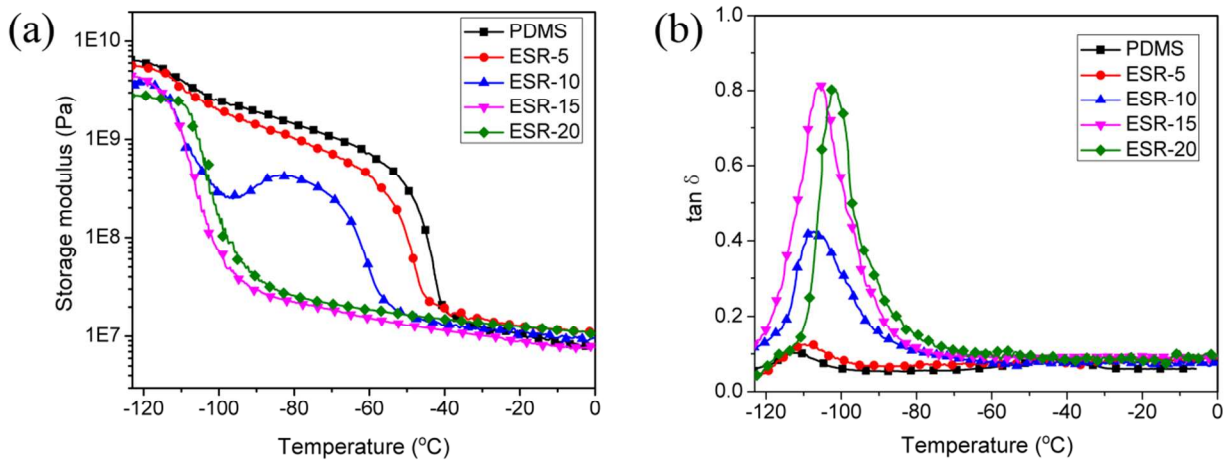

Fig. 9. Dynamic viscoelastic curves of PDMS composites and ESR composites: (a) storage modulus versus temperature; (b) *tanδ* versus temperature.

A material's *tanδ* designates the material's ratio of viscous to elastic components and is sometimes called the damping ability of the material.[57] Fig. 9(b) shows the *tanδ* of ESR composites with different epoxy contents versus temperature. Consistent with DSC results, the T_g of ESR composites obtained from the plot of *tanδ vs.* T increases with increasing epoxy content of ESR. The *tanδ* of ESR composites in the range -120–-80 °C increases significantly as the epoxy content of ESR increases. One possible reason for the increase of the *tanδ* is that the introduction of epoxy groups inhibits the crystallization of PDMS and the PDMS chains constrained by the crystals are able to move to lose energy. Another possible reason is that the epoxy groups on the side chains increase the friction between the macromolecular chains, resulting in an increase of energy loss during the segmental motions in the glass transition region.

Base on the DSC and DMA results, ESRs, especially ESR-15 and ESR-20, show excellent low-temperature performance and can be used as low-temperature-resistant materials. In practical applications, the cold resistance factor under compression (K_c) is often used to evaluate the low-temperature performance of a material. In this study, ESR composites with silica were prepared and the cold-resistance of ESR composites was investigated by using a cold-resistance-factor tester. The results, which are used to evaluate the low-temperature performance of ESR composites, are shown in Fig. 10. The cold resistance factor under compression is a measurement of the elasticity of a material, and the higher the K_c the higher the elasticity of the material. The K_c is influenced significantly by the T_g and crystallinity of the material. If a material has a T_g higher than the test temperature or easily crystallizes at the test temperature, the segmental motions will be inhibited and the material will have a low K_c. As shown in Fig. 10, all the composites have high K_c ($>$0.9) at room temperature and the difference in K_c between these composites is small, indicating that these composites have similar and very high elasticity. For the PDMS composite, the K_c is still high (K_c =0.67) at -50 °C, but begins to decrease significantly as the temperature decreases from -50 °C. At -60 °C, the K_c of the PDMS composite decreases to 0.31 because of the crystallization of PDMS. When the temperature decreases to -70 °C, the K_c of PDMS composite is almost 0, demonstrating that the PDMS composite has lost almost all its elasticity as a result of crystallization and cannot be used as an elastic material at temperatures lower than -70 °C. ESR-5 composite shows a better low-temperature performance than PDMS composite does and still remains highly elastic at -60°C. However, the K_c of ESR-5 composite decreases to only 0.11 at -70 °C, suggesting that the ESR-5 composite has also lost its elasticity at this temperature because of crystallization. The ESR composites with contents of epoxy groups higher than 9.21 mol% show high K_c at -50 °C, -60 °C, and -70 °C. Among these ESR composites (ESR-10, ESR-15, and ESR-20), ESR-10 composite shows the best low-temperature performance according to the K_c value, probably because it has the lowest T_g. As indicated by DMA results, however, ESR-15 composite and ESR-20 composite would show better low-temperature performance than ESR-10 composite does at temperatures lower than -70 °C due to the crystallization of ESR-10 in the temperature range -95–-80 °C. Because the cold-resistance-factor tester is cooled by dry ice, K_c values at a lower temperature than -70 °C cannot be obtained. Nevertheless, according to DSC and DMA results, we can confirm that these ESR composites, especially ESR-15 composite and ESR-20 composite, can be used as low-temperature-resistant materials at temperatures lower than -70 °C.

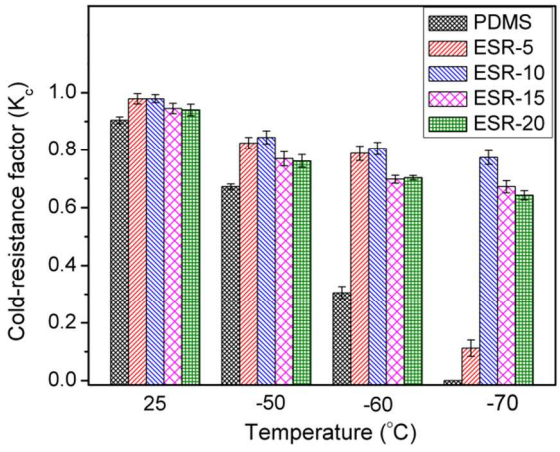

Fig. 10. Cold-resistance factors of PDMS composites and ESR composites at different temperatures.

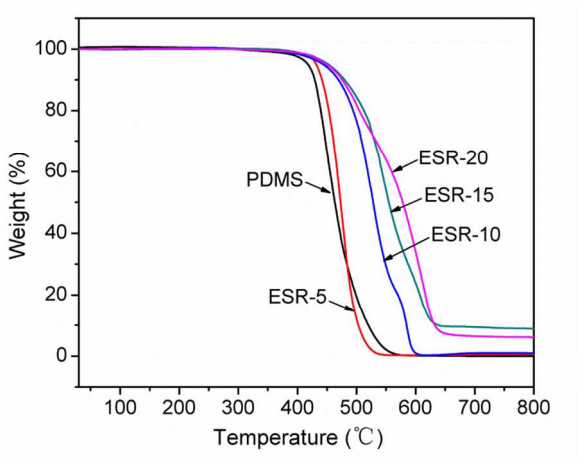

Fig. 11. TGA curves of PDMS and ESRs with different contents of epoxy groups.

In this study, we also studied the thermal stability and high-temperature applicability of ESR. Fig. 11 shows the TGA curves of uncured PDMS and uncured ESRs in inert atmosphere. It can be seen from these TGA curves that the thermal stability of ESR increases with increasing the content of epoxy groups. The temperature of 10% weight loss increases by 52 °C when 14.21 mol% of epoxy groups is introduced into the side chains of PDMS.

The thermal degradation of polysiloxane elastomer end-blocked with $(CH_3)_3Si$- groups in inert atmosphere can be explained by a well-known depolymerisation mechanism, as shown in Scheme 3.[6] When polysiloxane is heated in an inert atmosphere, silicone d-orbital participation is postulated with siloxane bond rearrangement, leading to the elimination of cyclic oligomers and the shortening of the residual chain length. The trimer cyclic oligomer is the most abundant product, with irregularly decreasing amounts of the tetramer, pentamer, and higher oligomers.[58] The transition state can be formed at any point of the silicone rubber chain, and the degradation process can take place continuously until the residual chain is too short to form cyclic oligomers.[59,60] Camino et al. suggested that the formation of cyclic transition is the rate-determining step during the thermal degradation.[60] In other words, the more easily the cyclic transition state forms, the weaker the thermal stability of silicone rubber is. Obviously, the flexibility of silicone rubber chains is the dominant factor for the thermal degradation. As confirmed by the increase of T_g, the flexibility of PDMS will decrease when polar epoxy groups are introduced into the side chains of PDMS. Therefore, the presence of epoxy groups will inhibit the formation of cyclic transition and increase the thermal degradation temperature. In addition, the steric hindrance of epoxy groups also inhibits the formation of cyclic transition.

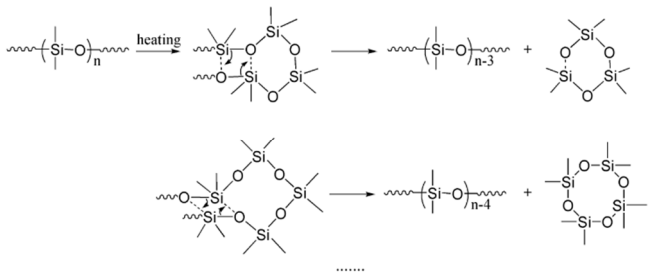

Scheme 3. Molecular mechanism for thermal degradation of polysiloxane.

Conclusions

A series of epoxidized polysiloxane (ESRs) with number-average molecular weights in the range 20,000–30,000 were successfully prepared by epoxidation of poly(methylvinylsiloxane) (SRs), which were synthesized by anionic ring-opening polymerization based on octamethyl cyclotetrasiloxane and 2,4,6,8-tetramethyl-2,4,6,8-tetravinyl cyclotetrasiloxane. The epoxidation of SR is a second-order reaction and the reaction rate constant decreases as the vinyl content of SR increases. More than 90% of the double bonds for the SRs could be converted into epoxy groups during the reaction at 25 °C for 96 h by using m-chloroperbenzoic acid (MCPBA). Although the glass transition temperature (T_g) of ESR increases slightly with increasing content of epoxy groups, ESR shows an improved low-temperature performance because the introduction of epoxy groups significantly inhibits the crystallization of polysiloxane. The ESR with 14.21 mol% of epoxy groups and a T_g of -116.2 °C was non-crystallizable and could remain elastic at -70 °C or lower. The very low T_g and non-crystallizability allow the use of ESRs as ideal low-temperature-resistant materials. ESRs also show higher thermal degradation temperatures in inert atmosphere than poly(dimethylsiloxane) does and can be used in high-temperature applications. This research suggests that an elastomer with both extremely low and high temperature resistance might be developed. In addition, the epoxy groups could act as chemical anchors for further chemical modification.

Acknowledgements

This work was financially supported by the Science Fund for Creative Research Groups of the National Natural Science Foundation of China (51221002) and the National Science Foundation for Distinguished Young Scholars (50725310).

Notes and references

[a] State Key Laboratory of Organic-Inorganic Composites, Beijing University of Chemical Technology, 100029, P. R. China. E-mail: zhanglq@mail.buct.edu.cn; Tel: +86 10 64423312.
[b] Key Laboratory of Beijing City for Preparation and Processing of Novel Polymer Materials, Beijing University of Chemical Technology, 100029, P. R. China. E-mail: zhanglq@mail.buct.edu.cn; Tel: +86 10 64423312.
[c] AVIC Beijing Institute of Aeronautical Materials, 100095, P. R. China. E-mail: jenny.wzh@163.com.

† Electronic Supplementary Information (ESI) available: the photographs of SR and ESR; ^{1}H NMR spectra of SRs and ESRs; thermal properties of PDMS, SRs and ESRs; and the DSC cooling curves of ESRs (cooling rate: 1°C/min). See DOI: 10.1039/b000000x/.

1 J. E. Mark, Acc. *Chem. Res.*, 2004, **37**, 946–953.
2 E. Pouget, J. Tonnar, P. Lucas, P. Lacroix-Desmazes, F. Ganachaud and B. Boutevin, *Chem. Rev.*, 2010, **110**, 1233–1277.
3 K. Chenoweth, S. Cheung, A. C. T. van Duin, W. A. Goddard and E. M. Kober, *J. Am. Chem. Soc.*, 2005, **127**, 7192–7202.
4 J. E. Mark, *in Silicones and Silicone-Modified Materials*, American Chemical Society, Washington DC, 2000.
5 V. Bartzoka, M. R. McDermott and M. A. Brook, *Adv. Mater.*, 1999, **11**, 257–259
6 F. B. Madsen, I. Dimitrov, A. E. Daugaard, S. Hvilsted and A. L. Skov, *Polym. Chem.*, 2013, **4**, 1700–1707.

7 Y. Meng, Z. Wei, L. Liu, L. Liu, L. Q. Zhang, T. Nishi and K. Ito, *Polymer*, 2013, **54** 3055–3064.
8 M. Petr, B. Katzman, W. DiNatale and P. T. Hammond, *Macromolecules*, 2013, **46**, 2823–2832.
9 W. Zhao, P. Fonsny, P. FitzGerald, G. G. Warra and S. Perrier. *Polym. Chem.*, 2013, **4**, 2140–2150.
10 L. Yang, Y. L. Lin, L. S. Wang and A. Q. Zhang, *Polym. Chem.*, 2014, **5**, 153–160.
11 K. E.Polmanteer and M. J. Hunter, *J. Appl. Polym. Sci.*, 1959, **1**, 3–10.
12 P.R. Sundararajan. Crystalline morphology of poly(dimethylsiloxane). *Polymer,* 2002, **43**, 1691–1693.
13 A.C.M. Kuo, *in Polymer data handbook: poly(dimethylsiloxane)*, Oxford University Press, Oxford, 1999.
14 V. Rajendra, Y. Chen and M. A. Brook, *Polym. Chem.*, 2010, **1**, 312–320.
15 M. Bračič,T. Mohan, R. Kargl,T. Griesser, S. Hribernik, S. Köstler, K. Stana-Kleinschek and L. Fras-Zemljič, *RSC Adv.*, 2014, **4**, 11955–11961.
16 J. G. Alauzun, S. Young, R. D'Souza, L. Liu, M. A. Brook and H. D. Sheardown, *Biomaterials*, 2010, **31**, 3471–3478.
17 K. Y. Chumbimuni-Torres, R. E. Coronado, A. M. Mfuh, C. Castro-Guerrero, M. Fernanda Silva, G. R. Negrete, R. Bizios and C. D. Garcia. *RSC Adv.*, 2011, **1**, 706–714.
18 P. J. Wipffa, H. Majda, C. Acharya, L. Buscemi, J. J. Meister and B. Hinz. *Biomaterials*，2009, **30**, 1781–1789.
19 Q. Xu, M. L. Pang, L. X. Zhu, Y. Y. Zhang and S. Y. Feng, *Mater. Des.*, 2010, **31**, 4083–4087.
20 A. Ghosh, P. P. De, S. K. De, M. Saito and V. Shingankuli, *Kautsch. Gummi Kunstst.*, 2003, **56**, 96–100.
21 Q. Wang, X. Zhang, L. Wang and Z. Mi, *J. Mol. Catal. A: Chem.*, 2009, **309**, 89–94.
22 Q. Wang, X. Zhang, L. Wang and Z. Mi, *Ind. Eng. Chem. Res.*, 2009, **48**, 1364–1371.
23 M. M. A. Nikje, A. Rafiee and M. Haghshenas, *Des. Monomers Polym.*, 2006, **9**, 293-303.
24 J. H. Bradbury and M. C. S. Pereral, *Ind. Eng. Chem. Res.* 1988, **27**, 2196–2203.
25 I. Kuźniarska-Biernacka, C. Pereira, A. P. Carvalho, J. Pires and C. Freire, *Appl. Clay Sci.*, 2011, **53**, 195–203.
26 D. Yang, *Acc. Chem. Res.*, 2004, **37**, 497–505.
27 V. Tanrattanakul, B. Wattanathai, A. Tiangjunya and P. Muhamud, *J. Appl. Polym. Sci.*, 2003, **90,** 261–269.
28 C. K. L. Davies and S. V. Wolfe, *Polymer*, 1983, **24**, 107–113.
29 N. Yamada, S. Shoji, H. Sasaki, A. Nagatani, K. Yamaguchi, S. Kohjiya and A. S. Hashim, *J. Appl. Polym. Sci.*, 1999, **71**, 855–863.
30 K. Jiamjitsiripong and C. J. Pattamaprom, *Elastom. Plast.*, 2011, **43**, 341–355.
31 T. L. A. C. Rocha, R. H. Schuster, M. M. Jacobi and D. Samios, *Kautsch. Gummi Kunstst.,* 2004, **57**, 656–661.
32 A. K. Manna, P. P. De, D. K. Tripathy, S. K. De and D. G. Peiffer, *J. Appl. Polym. Sci.*, 1999, **74**, 389–398.
33 W. H. Park, R. W. Lenz and S. Goodwin, *Macromolecules*, 1998, **31**, 1480–1486.
34 Z. Wang, X. Zhang,; R. G. Wang, H. L. Kang, B. Qiao, J. Ma, L. Q. Zhang and H. Wang, *Macromolecules*, 2012, **45**, 9010–9019.
35 F. L. Barcia, T. P. Amaral and B. G. Soares, *Polymer*, 2003, **44**, 5811.
36 R. Acosta Ortiz, M. L. G. Cisneros, G. A. García, Polymer, 2005, 46, 10663-10671.
37 J. M. Frances, G. Wajs, U.S. Patent 4,940,751, 1990-7-10.
38 W. E. Elias, K. S. Y. Lau, S. L. Oldham, U.S. Patent 4,788,268, 1988-11-29.
39 C. H. Lin, S. C. Huang, H. T. Li, U.S. Patent 8,440,774, 2013-5-14.
40 X.Yang, W. Huang, Y. Yu. Rubber Chem. Technol., 2011, 120, 1216-1224.
41 R. P. Eckberg, U.S. Patent 4,576,999, 1986-3-18.
42 J. N. Xin, P. Zhang, K. Huang and J. W. Zhang, *RSC Adv.*, 2014, **4**, 8525–8532.
43 K. Jaszcz and J. Lukaszczyk, *React. Funct. Polym.*, 2012, **72**, 650–656.
44 H. Hussain, A. Al-Harrasi, I. R. Green, I. Ahmed, G. Abbas and N. Ur Rehman. *RSC Adv.*, 2014, **4**, 12882–12917.
45 P. Zheng and T. J. McCarthy, *J. Am. Chem. Soc.*, 2012, **134**, 2024–2027.
46 P. R.Dluzneski, Rubber Chem. Technol., 2001, 74, 451-492.
47 J. Chojnowski and M. Cypryk, *in Silicon-Containing Polymers*, Kluwer Academic Publishers, Dordrecht, 2000.
48 P. Wichacheewa and A. E. Woodward, *J. Polym. Sci., Polym. Phys. Ed.*, 1978, **16**, 1849–1859.
49 P. D. Bartlett, *Rec. Chem. Prog.*, 1950, **11**, 47.
50 C. Kim, T. G. Traylor and C. L. Perrin, *J. Am. Chem. Soc.*, 1998, **120**, 9513–9516.
51 M. M. Jacobi, C. P. Neto, C. G. Schneider, T. L. A. C. Rocha and R. H. Schuster, *Kautsch. Gummi Kunstst.*, 2002, **55**, 590–595.
52 E. Delebecq, S. Hamdani-Devarennes, J. Raeke, J.-M. Lopez Cuesta and F. Ganachaud, *ACS Appl. Mater. Inter.*, 2011, **3**, 869–880.
53 J. Gearing, K. P. Malik and P. Matejtschuk, *Cryobiology*, 2010, **61**, 27–32.
54 G. Eising, A. Pauza and B. J. Kooi, *Cryst. Growth Des.*, 2013, **13**, 220–225.
55 S. Trabelsi, P. A. Albouy and J. Rault, *Macromolecules*, 2002, **35**, 10054–10061.
56 J. B. Le Cam and E. Toussaint, *Macromolecules*, 2010, **43**, 4708–4714.
57 M. G. Garrella, A. J. Shihb, B. M. Mac, E. Lara-Curziod and R. O. Scattergoode, *J. Magn. Magn. Mater.*, 2003, **257**, 32–43.
58 T. H. Thomas and T. C. Kendrick, *J. Polym. Sci., Part A-2*, 1969, **7**, 537–549.
59 G. Camino, S. M. Lomakin and M. Lageard, *Polymer*, 2002, **43**, 2011–2015.
60 G. Camino, S. M. Lomakin and M. Lazzari, *Polymer*, 2001, **42**, 2395–2402.

Captions of Figures and Tables:

Fig. 1. NMR spectra of poly(methylvinylsiloxane) (SR-20): (a) ^{1}H NMR spectrum and (b) ^{13}C NMR spectrum.

Fig. 2. NMR spectra of epoxy-poly(methylvinylsiloxane) (ESR-20): (a) ^{1}H NMR spectrum and (b) ^{13}C NMR spectrum.

Fig. 3. FTIR spectra of (a) D_4, (b) V_4, (c) SR-20, and (d) ESR-20.

Fig. 4. Epoxidation rate of SR samples with different vinyl contents.

Fig. 5. Plots of $\frac{1}{a-b}\ln\frac{b(1-w)}{a(b/a-w)}$ versus reaction time.

Fig. 6. DSC curves of PDMS and SRs with different contents of vinyl groups: (a) DSC cooling curves and (b) DSC heating curves.

Fig. 7. DSC curves of PDMS and ESRs with different epoxy values: (a) DSC cooling curves and (b) DSC heating curves.

Fig. 8. Plot of T_g against epoxy content of ESR.

Fig. 9. Dynamic viscoelastic curves of PDMS composites and ESR composites: (a) storage modulus versus temperature; (b) *tanδ* versus temperature.

Fig. 10. Cold-resistance factors of PDMS composites and ESR composites at different temperatures.

Fig. 11. TGA curves of PDMS and ESRs with different contents of epoxy groups.

Scheme 1. The synthesis route of ESR.

Scheme 2. The (a) rearrangement reaction and (b) chain transfer reaction during the synthesis of SRs.

Scheme 3. Molecular mechanism for thermal degradation of polysiloxane.